Investigation of J=1 states and their γ-decay behavior in ^{52}Cr

J. Wilhelmy, B. A. Brown, P. Erbacher, U. Gayer, J. Isaak, Krishichayan, B. Löher, M. Müscher, H. Pai, N. Pietralla, P. Ries, D. Savran, P. Scholz, M. Spieker, W. Tornow, V. Werner, and A. Zilges

Phys. Rev. C **98**, 034315 — Published 19 September 2018

DOI: 10.1103/PhysRevC.98.034315

Investigation of $J = 1$ states and their γ-decay behavior in ^{52}Cr

J. Wilhelmy,[1,*] A. Brown,[2] P. Erbacher,[3] U. Gayer,[4] J. Isaak,[4] Krishichayan,[5] B. Löher,[6] M. Müscher,[1] H. Pai,[7] N. Pietralla,[4] P. Ries,[4] D. Savran,[6] P. Scholz,[1] M. Spieker,[8] W. Tornow,[9,5] V. Werner,[4] and A. Zilges[1]

[1]*Institut für Kernphysik, Universität zu Köln, 50937 Köln, Germany*
[2]*Michigan State University, East Lansing, MI 48824-1321, USA*
[3]*Institute for Experimental Astrophysics, Goethe Universität Frankfurt, 60323 Frankfurt a.M., Germany*
[4]*Institut für Kernphysik, Technische Universität Darmstadt, 64289 Darmstadt, Germany*
[5]*Triangle Universities Nuclear Laboratory, Durham, North Carolina 27708, USA*
[6]*GSI Helmholtzzentrum für Schwerionenforschung GmbH, 64291 Darmstadt, Germany*
[7]*Saha Institute of Nuclear Physics, 1/AF, Bidhannagar, Kolkata 700064, India*
[8]*NSCL, Michigan State University, MI 48824, USA*
[9]*Department of Physics, Duke University, Durham, North Carolina 27708, USA*

(Dated: August 23, 2018)

Background: In the $A \approx 50$ mass region M1 spin-flip transitions are prominent around 9 MeV. An accumulation of 1^- states between 5 and 8 MeV generating additional E1 strength, also denoted as Pygmy Dipole Resonance (PDR), has been established in many nuclei with neutron excess within the last decade.
Purpose: The γ-decay behavior of J = 1 states has been investigated in an NRF experiment. M1 excitations have been compared to shell model calculations.
Methods: J = 1 states were excited by quasi-monoenergetic, linearly polarized γ-ray beams generated by Laser-Compton backscattering at the HIγS facility, Durham, NC, USA. Depopulating γ-rays were detected with the multi-detector array γ^3.
Results: For eleven beam-energy settings the γ-decay behavior of dipole states was analyzed by a state-to-state analysis and average γ-decay branching ratios have been investigated. 34 parity quantum numbers were assigned to $J = 1$ states.
Conclusions: Six 1^- states and two 1^+ states have been investigated in NRF experiments for the first time. The M1 strength distribution is in good agreement with shell-model calculations.

I. INTRODUCTION

Low-lying electric (E1) and magnetic (M1) dipole excitations are generated by different modes in atomic nuclei. It has been shown that for many nuclei a simple extrapolation of the Giant Dipole Resonance [1] to the low-energy region is not able to reproduce the low-lying E1 strength. Systematic investigations with various probes have been performed to study the structure of low-lying E1 strength [2]. An enhancement of low-lying E1 strength has been observed, e.g., in the Sn-isotopes [3–5], the $N = 82$ isotones [6–14], Ge-Isotopes [15], the $A \approx 90$ mass region [16–19], the $A \approx 130$ mass region [20, 21] and ^{208}Pb [22]. This accumulation of 1^- states between 5 and 8 MeV is commonly denoted as Pygmy Dipole Resonance (PDR). In a macroscopic picture, it can be associated with an oscillation of the neutron skin against the isospin-saturated core [2]. As this mode arises with increasing neutron excess, the PDR mode might have its onset in the $A \approx 50$ mass region. Whereas for the Ca-isotopes no enhanced E1 strength has been observed [23–25], in the Ni-isotopes low-lying E1 strength, which might be associated with the PDR, was identified [26, 27]. For further studies on ^{54}Cr the question arises, how the two valence neutrons affect the E1 strength. The complete data set on 1^- states including also weaker decay channels to excited states may provide crucial information on the onset of the PDR.

At around 9 MeV, M1 Gamow-Teller giant resonances are observed in the $A \approx 50$ mass region. These 1p-1h excitations across major closed shells correspond predominantly to the proton and neutron $1f_{7/2} \rightarrow 1f_{5/2}$ spin-flip excitation. For a systematic study of the evolution of magnetic dipole excitations in dependence of proton and neutron number in the $A \approx 50$ mass region several low-momentum transfer electron scattering experiments have been performed, e.g., on Ca-isotopes [28], $N = 28$ isotones [29], ^{46,48}Ti [30], and ^{58}Ni [31]. In most of these experiments, the assignment of spin and parity quantum numbers is not assured for many observed states. To further investigate the magnetic dipole strength distribution, complementary experiments with photons, that selectively excite $J = 1$ states, are very useful. Bremsstrahlung experiments with continuos photon flux have been performed for ^{40,44,48}Ca, ^{50,52}Cr, ^{56}Fe and ^{58,60}Ni [23–27, 32–35]. Additionally, for some of those nuclei, almost monoenergetic γ-ray beams from Laser-Compton backscattering (LCB) have been used [25–27, 35]. Most reliable systematic comparisons in the Cr-chain can be achieved by the same experimental approaches for each isotope. ^{52}Cr has already been investigated in bremsstrahlung experiments, but mainly ground-state transitions have been observed [34]. In bremsstrahlung experiments nonresonant scattered background is increasing towards lower energies in the spectrum which makes the observation of low-energy tran-

* wilhelmy@ikp.uni-koeln.de

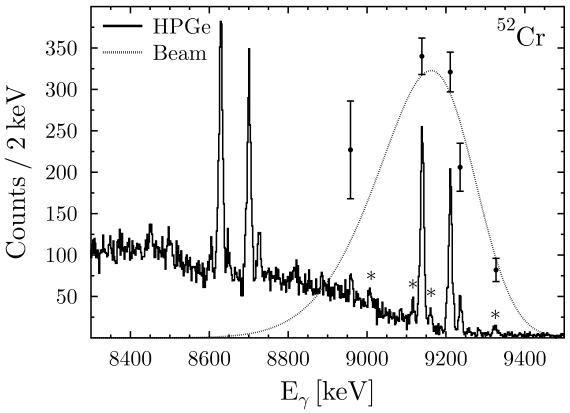

FIG. 1. The sum spectrum of all HPGe detectors for ^{52}Cr is depicted for a beam energy of 9.2 MeV. The γ-ray beam profile (dashed) and resolved peaks of ^{52}Cr with known cross sections to determine the absolute photon-flux distribution are illustrated. Additional $J = 1$ states that have not been observed in previous bremsstrahlung experiments are shown (*). The state at $E_x = 9009.4$ keV was observed for the first time in NRF experiments.

sitions quite difficult. Experiments with monoenergetic γ-ray beams are more sensitive to γ-decays to excited states and average branching ratios can be determined for every γ-beam energy setting [14, 21]. For the strongest $J = 1$ states parity quantum numbers have already been observed also in ^{52}Cr [36]. In this way, a systematic comparison with ^{50,54}Cr will be possible.

Here we present information on the γ-decay behavior of $J = 1$ states and weak excitations in ^{52}Cr from a Nuclear Resonance Fluorescence (NRF) experiment using almost mono-energetic γ-ray beams. The M1-strength distribution is compared to shell model calculations.

II. EXPERIMENTAL METHOD

The excitation in photon scattering experiments (γ,γ') is very selective on electric and magnetic dipole excitations in atomic nuclei. Excitation energies E_x, energy-integrated cross sections I_s, partial decay widths Γ_i and γ-decay branching ratios Γ_f/Γ can be deduced from NRF experiments [37]:

$$I_s = \pi^2 \cdot \left(\frac{\hbar c}{E_x}\right)^2 g \frac{\Gamma_0 \Gamma_f}{\Gamma} \qquad (1)$$

In the present experiment, the dipole response of ^{52}Cr was investigated using 100% linearly polarized and quasi-monoenergetic γ-ray beams generated by Laser-Compton backscattering at the High Intensity Gamma-ray Source (HIγS) facility at the Triangle Universities Nuclear Laboratory (TUNL), Durham, USA [38]. The dipole strength has been measured for twelve γ-ray beam energies at 5.5, 6.5, 6.7, 7.1, 7.3, 7.5, 7.7, 7.9, 8.1, 8.75, 9.2 and 9.4 MeV for about four hours each.

The γ-ray beam was collimated by a cylindrical lead collimator with a length of 30.5 cm and a radius of 9.525 mm on the ^{52}Cr target sample (99.54 % enriched) in oxide form with 1317.5 mg element weight. Primary and secondary de-exciting γ-rays were detected with the high-efficiency setup γ^3 [39]. This detector array consists of four $LaBr_3$:Ce (LaBr) scintillator detectors and four high-purity Germanium (HPGe) semi-conductor detectors. To enable the direct measurement of parity quantum numbers of $J = 1$ states, two detectors of each type were placed at $\theta = 90°$, one of each type in and one of each type out of the polarization plane. The other detectors were mounted under backward angles at $\theta = 135°$ (LaBr and HPGe at $\phi = \pm 45°$ and $\phi = \pm 135°$, respectively). θ denotes the scattering angle with respect to the beam axis and ϕ is the azimuthal angle.

The experimental azimuthal asymmetry ϵ of scattered photons is given by [8, 37]:

$$\epsilon = \frac{I_\parallel - I_\perp}{I_\parallel + I_\perp} = q\Sigma. \qquad (2)$$

$I_\parallel$ and $I_\perp$ denote the efficiency-corrected γ-ray intensities in the detectors parallel and perpendicular to the plane of polarization and q is the sensitivity of the setup. Because of the detectors' solid angle, the experimental asymmetry ϵ is not ± 1, but is equal to +0.82 for $J^\pi = 1^+$ states and -0.88 for $J^\pi = 1^-$ states.

Furthermore, intensities $I_\parallel$ and $I_\perp$ yield information on $E2/M1$ multipole-mixing ratios δ, i.e., for the transition $1^+ \rightarrow 2^+$. Detailed information can be found, e.g., in Refs. [40, 41].

The photon flux distribution of the γ-ray beam was directly measured with a 123% HPGe detector (beam detector) that can be moved in the beam line behind the γ^3 setup. The absolute photon flux $N_\gamma(E)$ is normalized to integrated scattering cross sections I_s of nuclear states known from a previous bremsstrahlung experiment [37] via:

$$N_\gamma(E_\gamma) = \frac{A}{\epsilon_{abs} \cdot N_T \cdot W(\theta,\phi) \cdot I_s} \qquad (3)$$

A denotes the peak area, ϵ_{abs} the absolute full-energy efficiency, N_T the number of target nuclei and $W(\theta,\phi)$ the angular distribution of the de-exciting γ-ray.

Fig. 1 shows as an example the spectrum and beam profile for a beam energy of 9.2 MeV. The absolute value of the photon flux is normalized to the largest scattering cross sections which were already measured in the bremsstrahlung experiment.

III. DATA ANALYSIS AND RESULTS

The experimental results are listed in tables I and II, for 1^+ states and 1^- states, respectively.

TABLE I. Associated excitation energies E_x and transition energies E_γ for 1^+ states of ^{52}Cr. Measured experimental asymmetries ϵ, spin and parity quantum numbers J^π, energy-integrated cross sections $I_{i,0}$, γ-decay branching ratios Γ_i/Γ_0, multipole-mixing ratios δ, and $B\,(M1)\uparrow$ values are given.

E_x (keV)	E_γ (keV)	ϵ	J^π	$I_{i,0}$ (eV · b)	Γ_0 (eV)	Γ_i/Γ_0	Γ_i/Γ_0 [e]	δ [a]	$B\,(M1)\uparrow$ [b] (μ_N^2)	$B\,(M1)\uparrow$ [c] (μ_N^2)	$B\,(M1)\uparrow$ [d] (μ_N^2)
6752.0(5)	6752.2(5)	+0.81(13)	1^+	22.3(24) [a]	0.174(25)				0.147(21)		
	5317.7(5)					0.44(14)					
	4104.3(5)					0.52(13)					
7166.2(5)	7165.7(5)	+1.00(51)	1^+	12.0(24) [e]	0.054(11)				0.038(8)	0.121(72)	
7524.1(5)	7523.6(5)	+0.69(10)	1^+	81.1(56) [e]	0.400(28)				0.244(18)	0.221(37)	1.3(2)
7825.6(5) [k]	7825.1(5)	+1.00(92)	1^+	13.1(19)	0.223(89)				0.121(49)	0.111(30)	
	6391.0(5)					2.2(10)		$0.17^{+0.19}_{-0.21}$			
7865.3(5)	7864.8(5)	+0.89(4)	1^+	80.9(51) [e]	0.470(41)				0.251(22)	0.293(31)	0.76(14)
	4900.2(5)					0.08(2)					
8014.6(10)	8015.0(10)	+0.60(19)	1^+	30.2(50) [e]	0.257(54)				0.129(32)		0.091(17)
	6579.1(5)					0.52(20)	0.54(16)				
8402.3(8) [j]	8401.6(8)									0.231(33)	0.12(2)
8581.9(10)	8582.0(10)	+0.45(16)	1^+	126(20)	1.12(19)				0.462(78)	0.143(25) [f]	0.12(2)
	7146.5(5)					0.30(13)					
9140.8(10)	9140.0(10)	+0.85(3)	1^+	364(21) [e]	2.65(14)				0.898(53)	1.118(59)	0.81(18)
9212.6(10)	9211.5(10)	+0.84(4)	1^+	286(19) [e]	2.30(15)				0.763(50)	0.879(50)	0.79(8)
	7778.2(5)					0.09(2)		$-0.04^{+0.23}_{-0.35}$			
9326.4(10)	9325.5(10)	+0.59(11)	1^+	99(11) [e]	0.746(80)				0.238(26)	0.235(32)	0.14(2)
9427.7(10)	9426.8(10)	+0.85(5)	1^+	123(15) [e]	0.95(11)				0.295(35)	0.339(50)	0.087(11)
9453.9(10) [k]	9453.0(10)	+0.84(9)	1^+	46.7(78)	0.363(60)				0.112(19)	0.199(36) [g]	
									$\Sigma\,3.70(14)$	$\Sigma\,3.89(14)$ [h]	$\Sigma\,4.22(31)$ [i]

[a] mixing ratio given in the phase convention of Krane and Steffen [42].
[b] calculated from Γ_0.
[c] electron scattering data, taken from Ref. [29].
[d] from Ref. [43], $\Gamma_i/\Gamma_0 = 0$ was assumed for all states in that work.
[e] bremsstrahlung data, taken from Ref. [34].
[f] energy 8600(10) keV in Ref. [29].
[g] energy 9440(20) keV in Ref. [29].
[h] lowest excitation observed in Ref. [29] and this experiment was $E_x = 7165.7$ keV. Only $J = 1$ states that have been observed in the present work and Ref. [29] are considered.
[i] lowest excitation observed in Ref. [43] was $E_x = 7523.1$ keV.
[j] no beam setting with energies between 8.1 MeV and 8.75 MeV in this experiment.
[k] newly discovered in the present work.

With the absolute photon flux $N_\gamma\,(E)$, integrated scattering cross sections I_s of states that were not observed in previous experiments were determined. Example given, for the beam energy of 9.2 MeV, the scattering cross sections of the state at $E_x = 9009.4$ keV was measured for the first time, while the states at 8960.4, 9140.8, 9212.6, 9238.2, and 9326.4 keV were used for the normalization, see Fig. 1. In total, two 1^+ states and six 1^- states were observed for the first time in NRF experiments.

The measured experimental asymmetries ϵ for all states that were observed in the present work are shown in Fig. 2. If an isolated transition was observed only either in the polarization plane of the incident γ-ray beam or perpendicular to it then an upper limit for the intensity in the other respective plane is specified.

In Fig. 3, the spectra of de-exciting γ-rays at a beam energy of 7.1 MeV are shown for the HPGe detectors parallel and vertical to the plane of polarization. Additionally, the spectrum that was measured under backward angles, where the angular distribution for E1 and M1 transitions to the 0^+ (-ground state) is identical, is shown. The figure illustrates the clear assignment of the electromagnetic type of radiation: The transitions in ^{52}Cr at 7013.4 and 7091.1 keV are of E1 nature. The two transitions at 6915.5 keV (2_1^+ in ^{16}O) and 6922.6 keV (1^- state in ^{52}Cr) form a double-peak structure as it is depicted in (c) of Fig. 3 for backward angles. Such a broad peak is also observed by Pai *et al.* [34] in previous NRF measurements with unpolarized bremsstrahlung.

At a γ-ray beam energy of 7.5 MeV a strong E1 tran-

TABLE II. Associated excitation energies E_x and transition energies E_γ for 1^- states of ^{52}Cr. Measured experimental asymmetries ϵ, spin and parity quantum numbers J^π, energy-integrated cross sections $I_{i,0}$, γ-decay branching ratios Γ_i/Γ_0, and $B\,(E1)\uparrow$ values are given.

E_x (keV)	E_γ (keV)	ϵ	J^π	$I_{i,0}$ (eV · b)	Γ_0 eV	Γ_i/Γ_0	Γ_i/Γ_0 [a]	$B\,(E1)\uparrow$ [b] $10^{-3}e^2\mathrm{fm}^2$	$B\,(E1)\uparrow$ [c] $10^{-3}e^2\mathrm{fm}^2$
5545.4(5)	5545.1(5)	−0.86(4)	1^-	41.9(25)[a]	0.112(7)			1.88(12)	
6460.6(5)	6461.6(5)	−0.85(7)	1^-	20.3(20)[a]	0.137(16)			1.45(17)	
	5025.9(5)					0.62(24)			
	3812.5(5)					0.23(7)			
6495.3(5)	6495.5(5)	−0.95(4)	1^-	35.6(25)[a]	0.158(14)			1.65(14)	
	5059.6(5)					0.14(6)			
	3849.1(5)					0.07(3)			
6691.6(5)[d]	6691.2(5)	−1.00(30)	1^-	16.5(44)	0.064(17)			0.62(16)	
6923.8(5)[d]	6922.6(5)	−1.00(91)	1^-	39.8(75)	0.209(41)			1.81(35)	
	5490.2(5)					0.24(7)			
7014.7(5)	7013.4(5)	−1.00(44)	1^-	39.5(44)[a]	0.218(29)			1.78(21)	
	5581.0(5)					0.29(9)	0.24(6)		
7089.8(5)	7091.1(5)	−1.00(31)	1^-	14.1(25)[a]	0.079(21)			0.63(17)	
	4440.9(5)					0.28(7)			
7252.3(5)[d]	7252.9(5)	−1.00(66)	1^-	13.2(33)	0.060(15)			0.45(12)	
7397.9(5)	7399.0(5)	−0.67(17)	1^-	22.5(32)[a]	0.157(21)			1.12(15)	
	4749.2(5)					0.47(12)			
7581.0(5)[d]	7580.4(5)	−0.80(8)	1^-	62.8(115)	0.314(58)			2.01(38)	
7732.3(5)	7731.7(5)	−0.87(4)	1^-	185(12)[a]	1.037(66)			6.44(46)	10.2(13)
7898.4(5)	7897.9(5)	−0.93(1)	1^-	623(32)[a]	3.45(18)			20.3(10)	24.3(17)
	4736.4(5)					0.02(1)			
8091.4(10)	8091.7(10)	−0.89(4)	1^-	128.8(78)[a]	1.01(10)			5.44(56)	3.4(4)
	6655.9(5)					0.37(11)			
8179.1(10)	8179.3(10)	−1.00(37)	1^-	36.3(58)[a]	0.55(13)			2.88(68)	2.7(5)
	6743.6(5)					1.6(8)	3.26(50)		
8217.7(10)	8217.0(10)	−1.00(62)	1^-	4.7(18)	0.028(10)			0.14(5)	0.27(12)
8706.0(10)[d]	8707.1(10)	−1.00(20)	1^-	17.1(55)	0.40(25)			1.7(11)	
	7269.4(5)					2.5(14)			
8763.1(10)	8762.3(10)	−0.77(16)	1^-	66.0(56)[a]	0.441(37)			1.88(16)	2.4(3)
8960.4(10)	8959.6(10)	−1.00(93)	1^-	33.3(52)[a]	0.233(36)			0.93(15)	1.5(2)
9009.4(10)[d]	9008.5(10)	−1.00(97)	1^-	60(13)	0.422(93)			1.65(33)	
9117.1(10)	9116.5(10)	−1.00(87)	1^-	22.0(45)	0.215(47)			0.81(18)	0.47(7)
	7682.2(5)					0.56(28)			
9161.6(10)	9160.7(10)	−1.00(89)	1^-	29.4(53)	0.215(39)			0.80(14)	0.66(9)
9238.2(10)	9237.3(10)	−1.00(29)	1^-	67.8(74)[a]	0.503(55)			1.83(20)	1.4(1)
9282.6(10)	9280.6(10)	−0.73(18)	1^-	31.8(68)	0.60(15)			2.15(53)	0.22(5)
	7848.9(5)					1.4(7)			
								Σ 60.4(19)	Σ 47.5(23)

[a] data taken from Ref. [34].
[b] calculated from Γ_0.
[c] data taken from Ref. [43], $\Gamma_i/\Gamma_0 = 0$ was assumed for all states in that work.
[d] newly discovered in the present work.

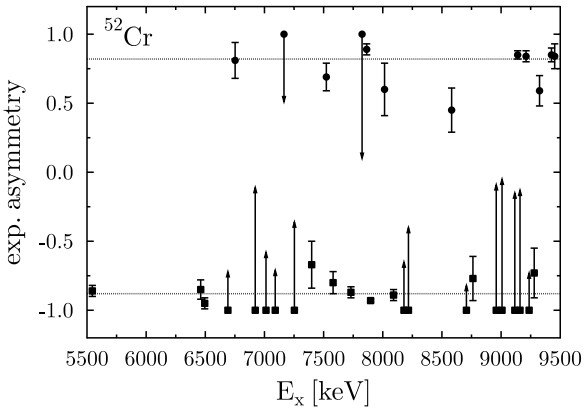

FIG. 2. Experimental asymmetry values and upper limits obtained for 1^- states (squares) and lower limits for 1^+ states (circles). Experimental sensitivities q are indicated by horizontally dashed lines (+0.82 and -0.88).

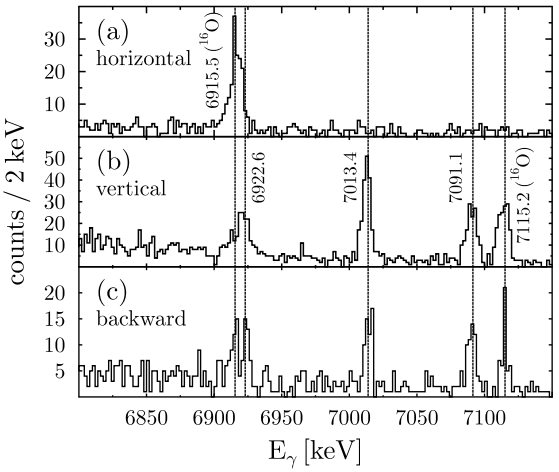

FIG. 3. HPGe spectra at 7.1 MeV γ-ray beam energy are shown for detectors positioned horizontal (a), vertical (b) and under backward angles ($\phi = \pm 45$ and $\theta = 135$) (c) with respect to the polarization plane. Transitions in ^{52}Cr at 6922.6 keV, 7013.4 keV, and 7091.1 keV are clearly of E1 nature.

sition at $E_\gamma = 7580.4(5)$ keV is seen. The observation of this de-excitation might have been concealed in previous bremsstrahlung measurements with continuous γ-ray fluxes by the single escape peak of the strong excitation at $E_\gamma = 8091.7(10)$ keV.

The 1^+ state at $E_x = 7825.6(5)$ shows a significant γ-decay branching of $\Gamma_{1^+\to 2_1^+}/\Gamma_0 = 2.2(10)$. Whereas the ground-state transition of this state was not observed in previous NRF experiments, the depopulating γ-ray into the 2_1^+ state was seen and erroneously assigned as a transition to the ground state. Pai *et al.* measured an intensity ratio of $W(90)/W(130) = 1.09(22)$ which supports the depopulation to a non spin-zero state. Additionally,

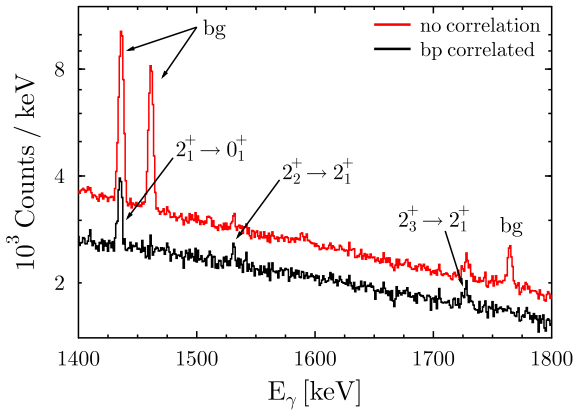

FIG. 4. (Color online) The low-energy part of the HPGe sum spectrum is shown at a γ-ray beam energy of 9.2 MeV. All events detected in the HPGe detectors are shown in red. The black spectrum shows only beam-pulse (bp) correlated events, the suppression of uncorrelated background is obvious. The depopulation of the first excited states $(2_1^+, 2_2^+, 2_3^+)$ are clearly visible.

the B($M1$) $\uparrow$ strength of this state that was extracted in the present work is in good agreement with the result of a low momentum-transfer electron scattering experiment, see table I.

In the present work, the depopulation of the 1^- state at $E_x = 6923.8$ keV to the 2_1^+ state was observed at 5490.2 keV. Enders *et al.* [44] erroneously assigned a transition at this γ-ray energy to a ground-state decay.

Three γ-decay branching ratios have been identified in previous bremsstrahlung experiments [34]. For the $J = 1$ states at $E_x = 7014.7$ keV ($\pi = -$) and $E_x = 8014.6$ keV ($\pi = +$) they are in very good agreement with the results of this work, see tables II and I, respectively.

At $E_x = 8179.1$ keV, the measured γ-decay branching ratio is higher by a factor of ≈ 2 in Ref. [34]. The intensity of the γ-decay to the 2_1^+ state might be too large in the previous bremsstrahlung experiment because of contributions from the single escape peak of the ground-state decay of the 1^- state at $E_x = 7252.3$ keV. This transition was previously unobserved.

Following the procedure in Refs. [14, 21, 26, 27] the intensities $I_{J_f^\pi}$ of the depopulating γ-rays from the first excited states J_f^π $(2_1^+, 0_2^+, 2_2^+, 2_3^+, 2_4^+)$ were determined from the HPGe spectra for every beam energy. The major part of the depopulation of $J = 1$ states that does not directly decay back to the groundstate is collected in these first excited states that serve like a funnel for their decay intensity. The intensities $I_{J_f^\pi}$ were then corrected for feeding contributions from secondary γ-rays, if observed, e.g., $I_{2_1^+}$ is corrected for $I_{0_2^+}$, because the 0_2^+ only decays to the 2_1^+.

Large background from the β^+ decay of ^{138}La at $E_\gamma = 1435.8$ keV contaminates the transition $2_1^+ \to 0_1^+$

(1434.1 keV) in ^{52}Cr. Therefore a background substraction is mandatory to determine $I_{2_1^+}$. In Fig. 4 all events detected in the HPGe sum spectrum at a beam energy of 9.2 MeV are shown in red. Gating on the beam-pick up signal of the γ-ray beam enables the selection of beam-pulse correlated events only (shown in black). The power of this method is obvious from the spectra, where the application of the beam-pulse coincidence (bpc) completely suppresses non-correlated background, e.g., at E_γ = 1460.8 keV (ϵ decay of ^{40}K), while the intensity $I_{2_1^+}$ emerges.

The intensity of the sum of all ground-state transitions of $J = 1$ states $I_{g.s.}$ was also determined by a state-to-state analysis for every beam energy. Hence, the average γ-decay branching ratios $I_{J_f^\pi}/I_{g.s.}$ for all $J = 1$ states were calculated for every beam-energy setting. The results are shown in table III.

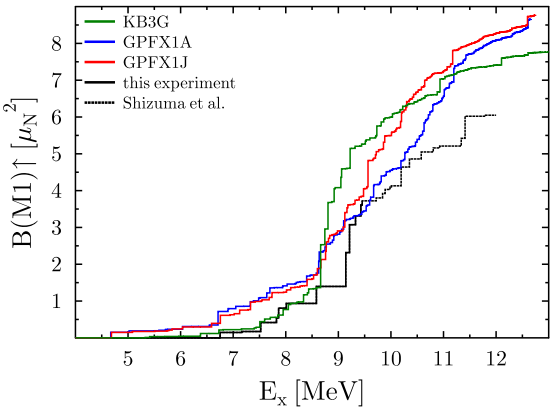

FIG. 5. (Color online) The B(M1)↑-strength distribution for shell-model calculations using the interactions KB3G (green), GPFX1A (blue), and GPFX1C (red) and experiments from this work (5.5 MeV to 9.5 MeV, solid black) and from Shizuma et al. (above 9.5 MeV, dashed black) are shown.

IV. DISCUSSION

A. E1-strength distribution

The total B($E1$)↑ strength observed in this work up to 9.9 MeV by state-to-state analysis amounts to $60.4(19) \times 10^{-3}\, e^2\mathrm{fm}^2$, which exhausts $\approx$ 0.2% of the Thomas-Reiche-Kuhn (TRK) sum rule. The four 1^- states at 7.732 MeV, 7.898 MeV, 8.091 MeV, and 8.179 MeV carry more than half of the total measured B($E1$)↑-strength. Similar concentration of E1-strength around 8 MeV has also been observed for the neighboring isotopes ^{54}Fe, ^{56}Fe and ^{58}Ni [32, 45]. The observed B($E1$)↑ strength in ^{52}Cr is about 20% higher by correcting for weak excitations and γ-decay branchings (determined from primary transitions, see table II) of 1^- states to excited states compared to the bremsstrahlung measurement of Pai *et al.* [34].

The average γ-decay branching ratios $I_{J_f^\pi}/I_{g.s.}$ from the depopulation of the first excited states never exceed 25% for every beam-energy setting above 7.1 MeV. This is a strong indication that almost no weak γ-decay branchings are unobserved from primary transitions. Furthermore, all three Cr isotopes have been investigated up to 9.9 MeV using bremsstrahlung and mono-energetic γ-ray beams, which make their experimental results comparable. Results on the E1-strength distribution of ^{50,54}Cr will be published soon.

The data situation for the E1-strength distribution along the N = 28 isotones is rather poor. For a systematic study of the evolution of the E1 strength with increasing proton number along the N = 28 isotones further NRF experiments have to be performed.

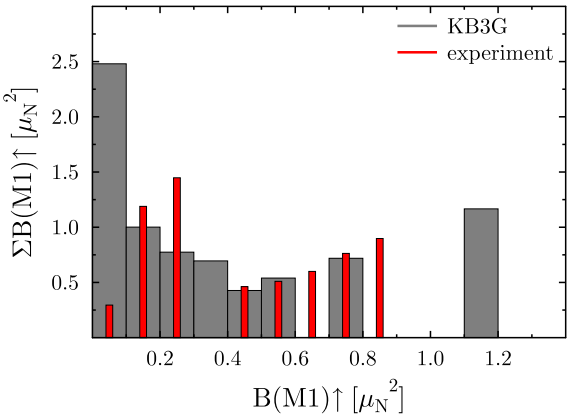

FIG. 6. (Color online) Summed M1 strength is shown for the data of this work (5.5 MeV to 9.5 MeV) together with the data from Shizuma *et al.* (9.5 MeV to 12 MeV) and the shell-model calculations using the KB3G interaction. The experimental data are indicated in red and the shell-model calculations in gray. Both are shown in bins of 0.1 μ_N^2.

B. Theoretical analysis of the M1-strength distribution

Excitation energies and B(M1)↑ values for the lowest 300 1^+ states were obtained from configuration-interaction calculations in the pf model space with the shell-model code NuShellX [46]. We used the effective Hamiltonians KB3G [47], GPFX1A [48] and GPFX1J [49]. Starting with GPFX1A, for GPFX1J the $f_{7/2} - f_{5/2}$ $T = 1$ two-body matrix elements where reduced by a factor of 0.7. This lowers the energy of the 1^+ state in ^{48}Ca that has a strong B(M1)↑ by 0.6 MeV, and reproduces its

TABLE III. Average γ-decay branching ratios Γ_f/Γ_0 for every beam-energy setting.

beam energy[a]		5.5	6.5	6.7	7.1	7.3	7.5	7.7	7.9	8.1	8.75	9.2	9.4
$I\left(1^+\right)/I\left(1^-\right)$[b]		0	0	1.16(18)	0.39(9)	1.45(17)	1.19(13)	0.39(6)	0.10(1)	0.20(6)	0.86(14)	3.13(32)	2.51(25)
E_f	J_f^π	$\frac{I_{J^\pi f}}{I_{g.s.}}$	$\frac{I_{J^\pi f}}{I_{g.s.}}$	$\frac{I_{J^\pi f}}{I_{g.s.}}$	$\frac{I_{J^\pi f}}{I_{g.s.}}$	$\frac{I_{J^\pi f}}{I_{g.s.}}$	$\frac{I_{J^\pi f}}{I_{g.s.}}$	$\frac{I_{J^\pi f}}{I_{g.s.}}$	$\frac{I_{J^\pi f}}{I_{g.s.}}$	$\frac{I_{J^\pi f}}{I_{g.s.}}$	$\frac{I_{J^\pi f}}{I_{g.s.}}$	$\frac{I_{J^\pi f}}{I_{g.s.}}$	$\frac{I_{J^\pi f}}{I_{g.s.}}$
(keV)		(%)	(%)	(%)	(%)	(%)	(%)	(%)	(%)	(%)	(%)	(%)	(%)
1434.1	2_1^+		31.8(19)	49.4(86)	0.3(4)	12.4(8)	3.9(12)	1.0(2)	0.4(1)	4.0(3)	12.4(22)	7.7(5)	3.9(3)
2646.9	0_2^+						8.2(4)			1.8(1)			
2964.8	2_2^+						6.0(3)	3.2(1)	0.7(1)	2.4(1)	6.8(6)	1.8(1)	3.1(1)
3161.7	2_3^+				4.3(3)		4.2(3)		1.2(1)		5.6(6)	2.8(1)	1.5(1)
3771.7	2_4^+											1.3(1)	1.0(1)
$\left(\sum_{f\neq 0}^N \frac{I_{J^\pi f}}{I_{g.s.}}\right)$			31.8(19)	49.4(86)	4.6(5)	12.4(8)	22.3(14)	4.2(3)	2.3(1)	8.3(3)	24.9(23)	13.6(5)	9.5(4)

[a] The value for the centroid energy of the beam-energy profile is given in MeV, the FWHM of the profile is about 3-5% depending on the energy.

[b] Intensity ratios of 1^+ to 1^- states are calculated from state-to-state analysis for all transitions observed at this beam energy.

observed energy of 10.23 MeV. For all of the calculated B(M1)↑, the spin g-factors were reduced by a factor of 0.74 [49].

For KB3G, GPFX1A and GPFX1J the energy of the strongest 1^+ state in ^{48}Ca is 9.3, 10.9 and 10.2 MeV, respectively, compared to the experimental value of 10.23 MeV (the KB3G strength is split between two states at 9.21 and 9.36 MeV). The calculated B(M1)↑ for the strong 1^+ states is 4.7, 4.9 and 5.5 μ_N^2, respectively, compared to experimental values of 3.9(3) μ_N^2 obtained with the (e,e′) reaction [28, 50] and 6.8(5) μ_N^2 obtained with the (γ,n) reaction [51]. The latter value was recently claimed to be inconsistent with data on (p,p′) reactions [52]. The total B(M1)↑ strength up to 13 MeV is 4.8, 5.8 and 5.8 μ_N^2, respectively, compared the experimental value of 5.1(3) μ_N^2 obtained with the (p,p′) reaction [53] and 5.3(6) μ_N^2 with the (e,e') reaction [50].

The calculations are compared to experiment in Fig. 5. Overall the agreement is good. KB3G does best in the excitation energy range of $4.0-8.5$ MeV. The position in energy of the increase above 8.5 MeV is correlated with the position of the calculated strong 1^+ state in ^{48}Ca given above.

Some strength to the weak states might be missed in this experiment. Therefore, for the KB3G shell-model calculations the fragmentation of the M1 strength is compared to the experiment, see Fig. 6. Here, all 1^+ states that have been observed are binned into $0.1\mu_N^2$ bins, e.g., the B(M1)↑ values for all 1^+ states with B(M1)↑ between 0.2 and 0.3 were added up which results in $\sum B\,(M1)\uparrow = 1.48$ for the bin with centroid $0.25\mu_N^2$ (for similar approaches see Ref. [10]). All M1 excitations with less than $0.1\,\mu_N^2$ contribute about $1.8\mu_N^2$ within the shell-model calculations but only $\approx 0.3\,\mu_N^2$ was observed from the experiments. It indicates that some M1 strength might be hidden in the continuum and is below the experimental sensitivity limit. This might increase the M1 strength observed in the experiment to higher values and might be reproduced also best by the KB3G interaction. Overall the KB3G describes the fragmentation of the experiment well for the stronger excitations.

At energies below 5.5 MeV no measurements at HIγS were performed, because no excitations were observed in previous bremsstrahlung measurements [34]. However, there also might be some weak M1 excitations hidden in the continuum.

Thus we expect the calculated strength to be higher than observed experimentally. The total calculated strength in ^{52}Cr of about 8 μ_N^2 is larger than the result for ^{48}Ca because both proton and neutron excitations from $f_{7/2}$ to $f_{5/2}$ contribute for ^{52}Cr, whereas only neutrons contribute to ^{48}Ca.

V. CONCLUSION

The low-lying dipole strength of ^{52}Cr has been investigated using almost mono-energetic γ-ray beams provided at the High Intensity γ-ray Source (HIγS). Two 1^+ states and six 1^- states have been observed for the first time in NRF experiments as well as several γ-decay branchings. Hence, the $\sum B(E1)\uparrow$ value from 5.5 MeV to 9.5 MeV increased about 20% compared to previous bremsstrahlung measurements and amounts to $60.4(19)\times 10^{-3}e^2\mathrm{fm}^2$, see table II.

The M1-strength distribution was compared to shell model calculations and the spin-g factors were reduced by a factor of 0.74. At lower energies no M1 strength is observed within the experiment and the shell model calculations. Between 8 MeV and 10 MeV strong M1 transitions are observed in this experiment and the shell-model calculations. The $\sum B(M1)\uparrow$ value amounts to $3.70(14)\mu_N^2$

from 5.5 MeV to 9.5 MeV from this work, see table I.

ACKNOWLEDGMENTS

We thank the HIγS operators for providing excellent γ-ray beams for our experiment. This work was supported by the BMBF (05P2015PKEN9 and 05P15RDEN9), the DFG (ZI 510/7-1 and SFB 1245), the Alliance Program of the Helmholtz Association (HA216/EMMI), as well as the Department of Energy, Office of Nuclear Physics under Grant No. DE-FG02-97ER41033. Julius Wilhelmy is supported by the Bonn-Cologne Graduate school.

[1] M. Harakeh and A. von der Woude, *Giant Resonances* (Oxford University Press, Oxford, 2001).
[2] D. Savran, T. Aumann, and A. Zilges, Prog. Part. Nucl. Phys. **70**, 210 (2013).
[3] H. K. Toft, A. C. Larsen, A. Bürger, M. Guttormsen, A. Görgen, H. T. Nyhus, T. Renstrøm, S. Siem, G. M. Tveten, and A. Voinov, Phys. Rev. C **83**, 044320 (2011).
[4] A. Krumbholz, P. von Neumann-Cosel, T. Hashimoto, A. Tamii, T. Adachi, C. Bertulani, H. Fujita, Y. Fujita, E. Ganioglu, K. Hatanaka, C. Iwamoto, T. Kawabata, N. Khai, A. Krugmann, D. Martin, H. Matsubara, R. Neveling, H. Okamura, H. Ong, I. Poltoratska, V. Ponomarev, A. Richter, H. Sakaguchi, Y. Shimbara, Y. Shimizu, J. Simonis, F. Smit, G. Susoy, J. Thies, T. Suzuki, M. Yosoi, and J. Zenihiro, Phys. Lett. B **744**, 7 (2015).
[5] A. Bracco, F. C. L. Crespi, and E. G. Lanza, Eur. Phys. J. A **51**, 99 (2015).
[6] R.-D. Herzberg, P. von Brentano, J. Eberth, J. Enders, R. Fischer, N. Huxel, T. Klemme, P. von Neumann-Cosel, N. Nicolay, N. Pietralla, V. Ponomarev, J. Reif, A. Richter, C. Schlegel, R. Schwengner, S. Skoda, H. Thomas, I. Wiedenhöver, G. Winter, and A. Zilges, Phys. Lett. B **390**, 49 (1997).
[7] R.-D. Herzberg, C. Fransen, P. von Brentano, J. Eberth, J. Enders, A. Fitzler, L. Käubler, H. Kaiser, P. von Neumann-Cosel, N. Pietralla, V. Y. Ponomarev, H. Prade, A. Richter, H. Schnare, R. Schwengner, S. Skoda, H. G. Thomas, H. Tiesler, D. Weisshaar, and I. Wiedenhöver, Phys. Rev. C **60**, 051307 (1999).
[8] N. Pietralla, Z. Berant, V. N. Litvinenko, S. Hartman, F. F. Mikhailov, I. V. Pinayev, G. Swift, M. W. Ahmed, J. H. Kelley, S. O. Nelson, R. Prior, K. Sabourov, A. P. Tonchev, and H. R. Weller, Phys. Rev. Lett. **88**, 012502 (2001).
[9] A. Zilges, S. Volz, M. Babilon, T. Hartmann, P. Mohr, and K. Vogt, Phys. Lett. B **542**, 43 (2002).
[10] D. Savran, M. Fritzsche, J. Hasper, K. Lindenberg, S. Müller, V. Y. Ponomarev, K. Sonnabend, and A. Zilges, Phys. Rev. Lett. **100**, 232501 (2008).
[11] D. Savran, M. Elvers, J. Endres, M. Fritzsche, B. Löher, N. Pietralla, V. Y. Ponomarev, C. Romig, L. Schnorrenberger, K. Sonnabend, and A. Zilges, Phys. Rev. C **84**, 024326 (2011).
[12] S. Volz, N. Tsoneva, M. Babilon, M. Elvers, J. Hasper, R. D. Herzberg, H. Lenske, K. Lindenberg, D. Savran, and A. Zilges, Nucl. Phys. A **779**, 1 (2006).
[13] B. Löher, D. Savran, T. Aumann, J. Beller, M. Bhike, N. Cooper, V. Derya, M. Duchêne, J. Endres, A. Hennig, P. Humby, J. Isaak, J. H. Kelley, M. Knörzer, N. Pietralla, V. Y. Ponomarev, C. Romig, M. Scheck, H. Scheit, J. Silva, A. P. Tonchev, W. Tornow, F. Wamers, H. Weller, V. Werner, and A. Zilges, Phys. Lett. B **756**, 72 (2016).
[14] A. P. Tonchev, S. L. Hammond, J. H. Kelley, E. Kwan, H. Lenske, G. Rusev, W. Tornow, and N. Tsoneva, Phys. Rev. Lett. **104**, 072501 (2010).
[15] T. Renstrøm, H.-T. Nyhus, H. Utsunomiya, R. Schwengner, S. Goriely, A. C. Larsen, D. M. Filipescu, I. Gheorghe, L. A. Bernstein, D. L. Bleuel, T. Glodariu, A. Görgen, M. Guttormsen, T. W. Hagen, B. V. Kheswa, Y.-W. Lui, D. Negi, I. E. Ruud, T. Shima, S. Siem, K. Takahisa, O. Tesileanu, T. G. Tornyi, G. M. Tveten, and M. Wiedeking, Phys. Rev. C **93**, 064302 (2016).
[16] C. Romig, J. Beller, J. Glorius, J. Isaak, J. H. Kelley, E. Kwan, N. Pietralla, V. Y. Ponomarev, A. Sauerwein, D. Savran, M. Scheck, L. Schnorrenberger, K. Sonnabend, A. P. Tonchev, W. Tornow, H. R. Weller, A. Zilges, and M. Zweidinger, Phys. Rev. C **88**, 044331 (2013).
[17] N. Benouaret, R. Schwengner, G. Rusev, F. Dönau, R. Beyer, M. Erhard, E. Grosse, A. R. Junghans, K. Kosev, C. Nair, K. D. Schilling, A. Wagner, and N. Benjaballah, Phys. Rev. C **79**, 014303 (2009).
[18] R. Schwengner, G. Rusev, N. Benouaret, R. Beyer, M. Erhard, E. Grosse, A. R. Junghans, J. Klug, K. Kosev, L. Kostov, C. Nair, N. Nankov, K. D. Schilling, and A. Wagner, Phys. Rev. C **76**, 034321 (2007).
[19] R. Schwengner, G. Rusev, N. Tsoneva, N. Benouaret, R. Beyer, M. Erhard, E. Grosse, A. R. Junghans, J. Klug, K. Kosev, H. Lenske, C. Nair, K. D. Schilling, and A. Wagner, Phys. Rev. C **78**, 064314 (2008).
[20] R. Massarczyk, R. Schwengner, F. Dönau, S. Frauendorf, M. Anders, D. Bemmerer, R. Beyer, C. Bhatia, E. Birgersson, M. Butterling, Z. Elekes, A. Ferrari, M. E. Gooden, R. Hannaske, A. R. Junghans, M. Kempe, J. H. Kelley, T. Kögler, A. Matic, M. L. Menzel, S. Müller, T. P. Reinhardt, M. Röder, G. Rusev, K. D. Schilling, K. Schmidt, G. Schramm, A. P. Tonchev, W. Tornow, and A. Wagner, Phys. Rev. Lett. **112**, 072501 (2014).
[21] J. Isaak, D. Savran, M. Krtička, M. W. Ahmed, J. Beller, E. Fiori, J. Glorius, J. H. Kelley, B. Löher, N. Pietralla, C. Romig, G. Rusev, M. Scheck, L. Schnorrenberger, J. Silva, K. Sonnabend, A. P. Tonchev, W. Tornow, H. R. Weller, and M. Zweidinger, Phys. Lett. B **727**, 361 (2013).
[22] A. Tamii, I. Poltoratska, P. von Neumann-Cosel, Y. Fujita, T. Adachi, C. A. Bertulani, J. Carter, M. Dozono, H. Fujita, K. Fujita, K. Hatanaka, D. Ishikawa, M. Itoh, T. Kawabata, Y. Kalmykov, A. M. Krumbholz, E. Litvinova, H. Matsubara, K. Nakanishi, R. Neveling, H. Okamura, H. J. Ong, B. Özel-Tashenov, V. Y. Ponomarev, A. Richter, B. Rubio, H. Sakaguchi, Y. Sakemi,

Y. Sasamoto, Y. Shimbara, Y. Shimizu, F. D. Smit, T. Suzuki, Y. Tameshige, J. Wambach, R. Yamada, M. Yosoi, and J. Zenihiro, Phys. Rev. Lett. **107**, 062502 (2011).
[23] T. Hartmann, J. Enders, P. Mohr, K. Vogt, S. Volz, and A. Zilges, Phys. Rev. C **65**, 034301 (2002).
[24] T. Hartmann, M. Babilon, S. Kamerdzhiev, E. Litvinova, D. Savran, S. Volz, and A. Zilges, Phys. Rev. Lett. **93**, 192501 (2004).
[25] J. Isaak, D. Savran, M. Fritzsche, D. Galaviz, T. Hartmann, S. Kamerdzhiev, J. H. Kelley, E. Kwan, N. Pietralla, C. Romig, G. Rusev, K. Sonnabend, A. P. Tonchev, W. Tornow, and A. Zilges, Phys. Rev. C **83**, 034304 (2011).
[26] M. Scheck, V. Y. Ponomarev, T. Aumann, J. Beller, M. Fritzsche, J. Isaak, J. H. Kelley, E. Kwan, N. Pietralla, R. Raut, C. Romig, G. Rusev, D. Savran, K. Sonnabend, A. P. Tonchev, W. Tornow, H. R. Weller, and M. Zweidinger, Phys. Rev. C **87**, 051304(R) (2013).
[27] M. Scheck, V. Y. Ponomarev, M. Fritzsche, J. Joubert, T. Aumann, J. Beller, J. Isaak, J. H. Kelley, E. Kwan, N. Pietralla, R. Raut, C. Romig, G. Rusev, D. Savran, L. Schorrenberger, K. Sonnabend, A. P. Tonchev, W. Tornow, H. R. Weller, A. Zilges, and M. Zweidinger, Phys. Rev. C **88**, 044304 (2013).
[28] W. Steffen, H. D. Gräf, W. Gross, D. Meuer, A. Richter, E. Spamer, O. Titze, and W. Knüpfer, Phys. Lett. B **95**, 23 (1980).
[29] D. I. Sober, B. C. Metsch, W. Knüpfer, G. Eulenberg, G. Küchler, A. Richter, E. Spamer, and W. Steffen, Phys. Rev. C **31**, 2054 (1985).
[30] A. Richter, Nucl. Phys. A **507**, 99c (1990).
[31] W. Mettner, A. Richter, W. Stock, B. C. Metsch, and A. G. Van Hees, Nucl. Phys. A **473**, 160 (1987).
[32] F. Bauwens, J. Bryssinck, D. DeFrenne, K. Govaert, L. Govor, M. Hagemann, J. Heyse, E. Jacobs, W. Mondelaers, and V. Y. Ponomarev, Phys. Rev. C **62**, 024302 (2000).
[33] K. Govaert, W. Mondelaers, E. Jacobs, D. De Frenne, K. Persyn, S. Pommé, M.-L. Yoneama, S. Lindenstruth, K. Huber, A. Jung, B. Starck, R. Stock, C. Wesselborg, R.-D. Heil, U. Kneissl, and H. Pitz, Nucl. Inst. and Meth. A **337**, 265 (1994).
[34] H. Pai, J. Beller, N. Benouaret, J. Enders, T. Hartmann, O. Karg, P. von Neumann-Cosel, N. Pietralla, V. Y. Ponomarev, C. Romig, M. Scheck, L. Schnorrenberger, S. Volz, and M. Zweidinger, Phys. Rev. C **88**, 054316 (2013).
[35] H. Pai, T. Beck, J. Beller, R. Beyer, M. Bhike, V. Derya, U. Gayer, J. Isaak, Krishichayan, J. Kvasil, B. Löher, V. O. Nesterenko, N. Pietralla, G. Martínez-Pinedo, L. Mertes, V. Y. Ponomarev, P. G. Reinhard, A. Repko, P. C. Ries, C. Romig, D. Savran, R. Schwengner, W. Tornow, V. Werner, J. Wilhelmy, A. Zilges, and M. Zweidinger, Phys. Rev. C **93**, 014318 (2016).
[36] Krishichayan, M. Bhike, W. Tornow, G. Rusev, A. P. Tonchev, N. Tsoneva, and H. Lenske, Phys. Rev. C **91**, 044328 (2015).
[37] U. Kneissl, H. H. Pitz, and A. Zilges, Prog. Part. Nucl. Phys. **37**, 349 (1996).
[38] H. R. Weller, M. W. Ahmed, H. Gao, W. Tornow, Y. K. Wu, M. Gai, and R. Miskimen, Prog. Part. Nucl. Phys. **62**, 257 (2009).
[39] B. Löher, V. Derya, T. Aumann, J. Beller, N. Cooper, M. Duchêne, J. Endres, E. Fiori, J. Isaak, J. Kelley, M. Knörzer, N. Pietralla, C. Romig, D. Savran, M. Scheck, H. Scheit, J. Silva, A. Tonchev, W. Tornow, H. Weller, V. Werner, and A. Zilges, Nucl. Inst. and Meth. A **723**, 136 (2013).
[40] G. Rusev, A. P. Tonchev, R. Schwengner, C. Sun, W. Tornow, and Y. K. Wu, Phys. Rev. C **79**, 047601 (2009).
[41] T. Beck, J. Beller, N. Pietralla, M. Bhike, J. Birkhan, V. Derya, U. Gayer, A. Hennig, J. Isaak, B. Löher, V. Y. Ponomarev, A. Richter, C. Romig, D. Savran, M. Scheck, W. Tornow, V. Werner, A. Zilges, and M. Zweidinger, Phys. Rev. Lett. **118**, 1 (2017).
[42] K. Krane, R. Steffen, and R. Wheeler, At. Data Nucl. Data Tables **11**, 351 (1973).
[43] T. Shizuma, T. Hayakawa, I. Daito, H. Ohgaki, S. Miyamoto, and F. Minato, Phys. Rev. C **96**, 044316 (2017).
[44] J. Enders, P. von Brentano, J. Eberth, R.-D. Herzberg, N. Huxel, H. Lenske, P. von Neumann-Cosel, N. Nicolay, N. Pietralla, H. Prade, J. Reif, A. Richter, C. Schlegel, R. Schwengner, S. Skoda, H. Thomas, I. Wiedenhöver, G. Winter, and A. Zilges, Nucl. Phys. A **636**, 139 (1998).
[45] T. Shizuma, T. Hayakawa, H. Ohgaki, H. Toyokawa, T. Komatsubara, N. Kikuzawa, T. Inakura, M. Honma, and H. Nakada, Phys. Rev. C **87**, 024301 (2013).
[46] B. A. Brown and W. D. M. Rae, Nucl. Data Sheets **120**, 115 (2014).
[47] A. Poves, J. Sánchez-Solano, E. Caurier, and F. Nowacki, Nucl. Phys. A **694**, 157 (2001).
[48] M. Honma, T. Otsuka, B. A. Brown, and T. Mizusaki, Eur. Phys. J. A **25**, 499 (2005).
[49] M. Honma, T. Otsuka, T. Mizusaki, M. Hjorth-Jensen, and B. A. Brown, J. Phys.: Conf. Ser. **20**, 7 (2005).
[50] W. Steffen, H.-D. Gräf, A. Richter, A. Härting, W. Weise, U. Deutschmann, G. Lahm, and R. Neuhausen, Nucl. Phys. A **404**, 413 (1983).
[51] J. R. Tompkins, C. W. Arnold, H. J. Karwowski, G. C. Rich, L. G. Sobotka, and C. R. Howell, Phys. Rev. C **84**, 044331 (2011).
[52] J. Birkhan, H. Matsubara, P. von Neumann-Cosel, N. Pietralla, V. Y. Ponomarev, A. Richter, A. Tamii, and J. Wambach, Phys. Rev. C **93**, 041302(R) (2016).
[53] M. Mathy, J. Birkhan, H. Matsubara, P. von Neumann-Cosel, N. Pietralla, V. Y. Ponomarev, A. Richter, and A. Tamii, Phys. Rev. C **95**, 054316 (2017).